Controlled Ionospheric Preconditioning and Stimulated Electromagnetic Radiation

P. Y. Cheung, A. Y. Wong, and J. Pau
Department of Physics and Astronomy, University of California, Los Angeles, California 90095

E. Mjølhus
Institute of Mathematical Sciences, University of Tromsø, N-9037 Tromsø, Norway
(Received 22 January 1998)

New results of stimulated electromagnetic emissions (SEE) from the HIPAS Observatory are reported. A novel hf heating sequence was used to first precondition the ionosphere, and SEE was then excited with low-amplitude test pulses. Through this approach, the nonlinear physics of SEE was studied. The correlation between small-scale field-aligned density striations and SEE generation was demonstrated, and SEE was excited at power density of 24 dB less than normally required. The results compare well with theoretical predictions of SEE generation via trapped upper hybrid oscillations decay and cavitation within striations. [S0031-9007(98)06204-8]

PACS numbers: 94.20.Tt, 52.35.Mw, 52.35.Ra

The ionosphere provides an "outdoor laboratory" [1] ideally suited for the study and excitation of thermal and nonlinear plasma instabilities through high frequency (hf) ionospheric modification experiments. A manifestation of thermal instabilities is the observation of magnetic field-aligned density striations detected via radar scattering [2–4] and *in situ* rocket measurements [5]. A manifestation of nonlinear plasma processes is the observation of stimulated hf radiation from the heated ionosphere, commonly called stimulated electromagnetic emissions (SEE), through frequency analysis of the returned hf signal after its transit through the ionosphere [6–16]. Two of the more robust SEE spectral features observed under high duty cycle hf heating are a broad, diffuse, and down-shifted (with respect to the heating frequency, f_{hf}) continuum, with frequency extension of tens of kilohertz or more, called the broad continuum; and a discrete, narrow, down-shifted peak, called the down-shifted maximum, with an offset frequency near the lower hybrid frequency, f_{lh} [11,12].

It has been suggested that these SEE features are associated with the occurrence of heater-induced small-scale (meter-size) striations [17–21] which act as resonators for electrostatic oscillations at the upper hybrid frequency, f_{uh}. In contrast to Langmuir oscillations near the reflection layer where $f_{\mathrm{hf}} \sim f_p(z_o)$ [$f_p(z_o)$ is the plasma frequency at the reflection layer z_o], these oscillations have wave vectors predominantly perpendicular to the ambient magnetic field. Recently, Mjølhus [22,23] proposes a SEE theory including the presence of striations and has calculated the radiation source current spectra. Trapped upper hybrid oscillations or eigenstates, with frequency of $f = f_{\mathrm{hf}} = f_{\mathrm{uh}}(z)$, are first generated via conversion of pump wave off meter-size striations. The parametric decay of these states, with $f' = f_{\mathrm{hf}} - f_{\mathrm{dm}}$ (f' is the decay wave frequency), results in the generation of the down-shifted maximum feature. Optimum growth of this trapped upper hybrid decay instability is predicted to occur when the frequency offset, f_{dm} ($f_{\mathrm{hf}} - f'$), is near f_{lh}. The resultant radiation source current spectrum contains discrete spectral peaks that can be identified with the down-shifted maximum feature. As the pump field increases, the discrete peaks change to a broad diffuse continuum. A new cavitation process within the striations has also been suggested for the generation of the broad continuum feature.

The physics of nonlinear SEE generation, in short, encompasses fundamental processes such as the conversion of electromagnetic waves to electrostatic waves off striations, the excitation of trapped eigenmodes, parametric instabilities, and stimulated radiation of electrostatic waves. These issues are topics of active research not only in ionospheric experiments but also in laboratory studies. It is of general interest and great importance, then, that these issues be studied in relation to SEE, that the correlation of striations and SEE be demonstrated, and that details of theoretical predictions be tested under controlled experiments. A survey of past experiments, however, yields inconclusive results.

In this Letter, new results of SEE from a series of controlled ionospheric preconditioning experiments are presented. Specifically, our experimental procedure allows (i) each heating sequence to initiate from or to approach that of a cold start condition; (ii) the complete history of temporal evolution of SEE, from its initial growth to its long-time evolution, be recorded; (iii) the correlation of striations and SEE be clearly demonstrated; and (iv) the low threshold requirement of SEE generation via the trapped upper hybrid decay instability and cavitation be verified. Our results demonstrate unambiguously that, in a preconditioned ionosphere with striations, SEE feature such as the down-shifted maximum can be excited and observed readily with test hf pulses that can be 24 dB weaker in power density than normally required without preconditioning. We have also found that the most dramatic data were observed under the conditions when hf

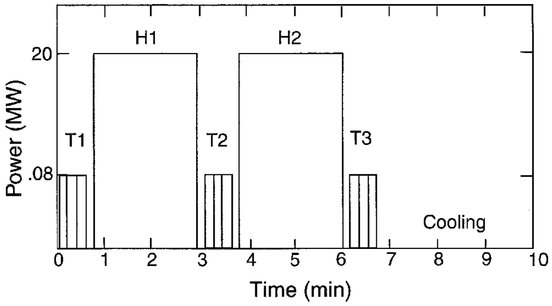

FIG. 1. Schematic of one heating sequence. The sequence consisted of a series of test pulses (T_1, T_2, and T_3) at an effective radiated power ~80 kW, two heating pump pulses (H_1 and H_2) at ~20 MW, and a cooling period.

heater pump frequency, f_{hf}, is near the maximum plasma frequency, $f_o F_2$, of the ionosphere [24,25].

To accomplish our objectives, a novel heating sequence was used instead of transmitting at maximum power continuously. Figure 1 shows one cycle of the heating sequence (10 min long) consisting of three series of short test pulses (T_1, T_2, and T_3), two main heating pump pulses (H_1 and H_2), and a long cooling period. Each series of test pulses further consisted of three separate pulses (10 s each) at three different test frequencies. Test pulses, T_1, were first transmitted to check the background ionospheric conditions and to ensure a cold start condition, i.e., a clean ionosphere with no prior heating effects. This was accomplished by monitoring the spectra of returned signals of test pulses at multiple frequencies. The duration of each pump pulse, 136 s, was chosen to facilitate the growth of small-scale (meter-size) striations while avoiding the excitation of larger scale perturbations. The effects of heating from the first pump pulse, H_1, were monitored by a second sequence of test pulses, T_2, and the effects of H_2, which can also be considered as a test pulse with large amplitude, were monitored by a final sequence of test pulses, T_3. The heating cycle was then repeated after the long cooling period of 200 s when all hf transmission was off.

Experiments were performed periodically from late February to early November 1997 at HIPAS Observatory [26]. The results presented here were selected from the June experiment and are representative of the overall data collected. Measurements of returned hf waves were made at the NOAA facility at Gilmore Creek, 33 km away from the HIPAS Observatory. For this particular set of experiments, the effective radiated power of the main heater wave was ~20 MW while that of the test pulses was ~80 kW. Both the transmitted main pump wave with $f_{\mathrm{hf}} = 4.53$ MHz and the test pulses with frequencies of $f_t = 4.50, 4.53$, and 4.56 MHz were at ordinary (O) mode polarization. These heating and test frequencies were near $f_o F_2$ but were sufficiently away from the nearest multiples of electron cyclotron frequency f_{ce} that gyroharmonic effects are minimized [10]. Specifically, $(f_{\mathrm{hf}}, f_t) - 3f_{ce} > 300$ kHz at the reflection layer of ~220 km.

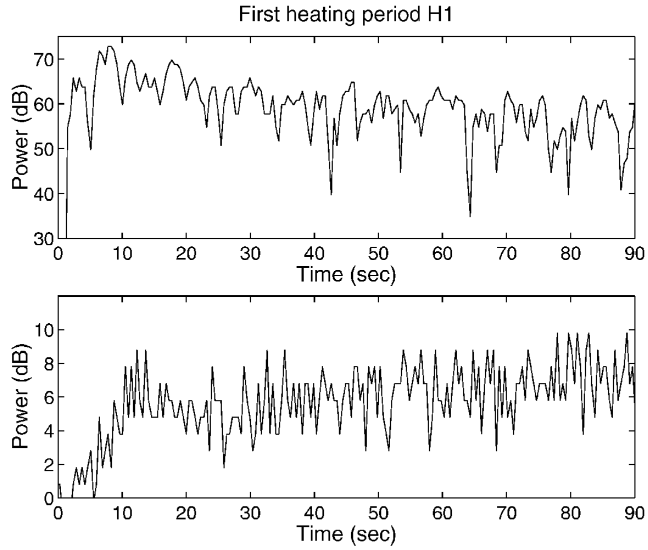

FIG. 2. Temporal evolution of returned hf signal of the first pump pulse H_1 which shows a gradual decline (top panel) and the SEE signal at -9 kHz from f_{hf} which shows a gradual increase (bottom panel).

The temporal evolution of the returned hf power of pump H_1 and its spectral (or SEE) power at a down-shifted frequency of -9 KHz are shown in Fig. 2. Cold start condition was first confirmed by monitoring the return of T_1 [see Fig. 4(a)]. After turn-on at $t = 2$ s, the return pump signal (top panel) drop 10 dB from a range of ~72 dB to a range of ~62 dB within a span of 20 s. This drop in return pump strength is generally attributed to the anomalous absorption of the pump signal as a result of the formation of striations and the subsequent scattering and conversion of pump wave to electrostatic oscillations [10,27–29]. The SEE signal at -9 kHz (bottom panel), on the other hand, displays a rapid rise within the first 10–15 s after turn-on. These two figures clearly show that the growth of SEE is correlated with the decline of pump signal and the excitation of striations.

Sample spectra of returned hf signal of pump H_1 at two discrete times, one near turn-on and the other 88 s into the heating pulse, are shown in Figs. 3(a) and 3(b), respectively. Following past convention, the broad diffuse structure extending from the pump signal peak to negative frequencies is labeled the broad continuum, while the broad peak riding on the continuum at about 9–10 kHz is labeled the down-shifted maximum. The center frequency of the down-shifted maximum feature is close to the lower hybrid frequency of $f_{\mathrm{lh}} \sim 8$ kHz. Comparison of Figs. 3(a) and 3(b) illustrates the relatively slow growth of SEE during this first heating period initiating from cold start. For this set of data, the down-shifted maximum feature is barely noticeable in Fig. 3(b).

Preconditioning by pump H_1 makes a significant impact on subsequent test pulse results. This is illustrated by the difference in SEE spectra of returned signals of test pulses T_1 and T_2 before and after H_1 shown

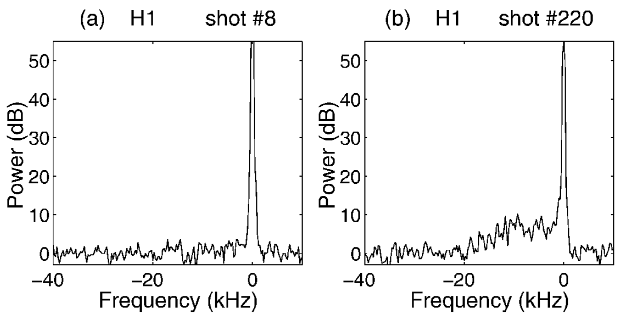

FIG. 3. Frequency spectra of returned hf signal of first pump pulse H_1. Panel (a) shows the spectrum near turn-on of H_1. Panel (b) shows the spectrum 88 s into heating. The horizontal frequency scale is offset from f_{hf}.

in Figs. 4(a) and 4(b) for $f_t = 4.56$ MHz. Figure 4(a) shows, as expected, no SEE from the turn signal of T_1. This is consistent with the cold start condition and the result of the much reduced effective radiated power of 80 kW. After preconditioning, however, the results are very different. Figure 4(b) shows a sample spectrum from the return signal of T_2 transmitted 4 s after H_1 was turned off. First, good SEE was observed even at the reduced radiated power. Second, the spectrum shows a very strong and discrete down-shifted maximum feature. This is in distinct contrast to the down-shifted maximum features observed from main pump pulses H_1 and H_2 which are frequently superposed on a continuum background. The discreteness of the down-shifted maximum feature also appears to be more robust when $f_{\mathrm{hf}} \sim f_o F_2$.

Preconditioning effects can also persist past the turn-on time of second pump pulse H_2 (transmitted 44 s after H_1 is shut off), and the results are shown in Fig. 5. The returned power of H_2 (top panel), in contrast to that from H_1 shown in Fig. 2, is at a depressed level of $\sim$62 dB due to anomalous absorption from preexisting striations immediately at turn-on, and remains depressed throughout the heating period. The evolution of SEE power at -9 KHz (bottom panel) is also in contrast to that of H_1. It has a strong overshoot at turn-on which is followed by a quick drop with the signal level settling into the same range as that during H_1. This overshoot is very reproducible and occurs consistently during the second heating period with the combination of a large heating pump and preexisting striations.

The overshoot also leads to large frequency broadening in SEE spectra of return signal of second pump H_2. Figure 6(a) shows the spectrum during the overshoot. It shows strong SEE that has a relatively sharp down-shifted maximum peak riding on top of a very broad continuum with frequency extension of over 30 kHz. Figure 6(b) shows the spectrum 9 s into the heating period. It shows weaker SEE with a broader down-shifted maximum peak riding on a much narrower continuum background. Comparison of the two sets of spectra shown in Figs. 3 and 6 clearly contrasts the systematic growth of SEE from cold start condition with pump H_1 and the overshoot phenomenon of SEE with pump H_2 after preconditioning.

Many of our observed results can now be compared with theoretical predictions of Mjølhus [22,23] and be explained. First, the presence of meter-size striation is required in the model. As pointed out earlier, this is inferred experimentally with results from H_1 where the growth of the SEE signal is correlated with the anomalous decay of the pump signal [10,27–29]. Second, the model predicts a very low threshold for the excitation of trapped under hybrid decay instability. This is confirmed by our test pulses data that show the power threshold can be more than 20 dB lower with respect to H_1 and H_2 that generate the striations. Converting experimental parameters into the same scaled units as in the model and comparing with the instability threshold, the test

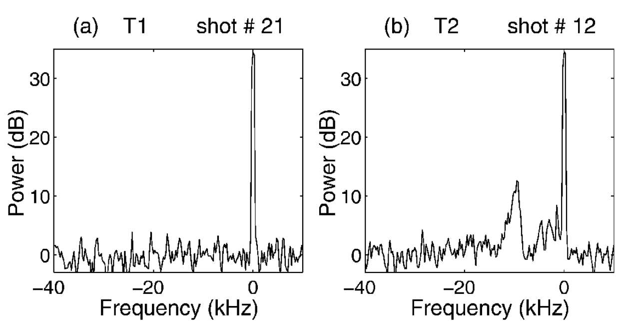

FIG. 4. Frequency spectra of returned signal of test pulses T_1 and T_2. Panel (a) shows no SEE for T_1 before H_1. Panel (b) shows SEE with a discrete down-shifted maximum feature for T_2 after H_1. The frequency scale on each panel is offset from $f_t = 4.56$ MHz.

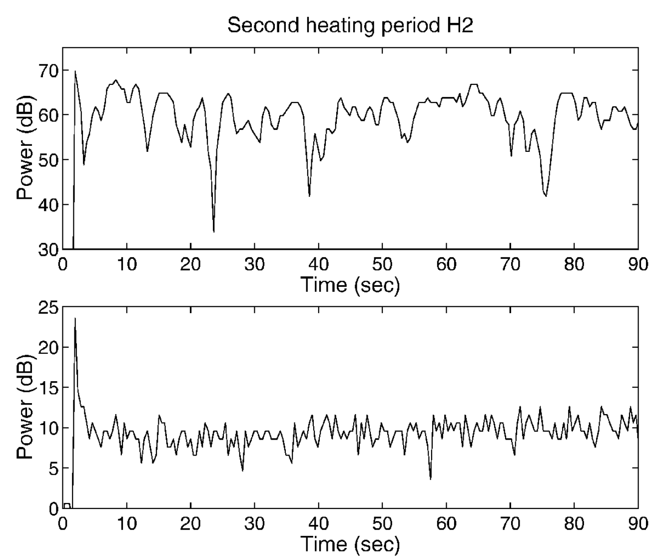

FIG. 5. Temporal evolution of returned hf signal of second pump pulse H_2 (top panel) and the SEE signal at -9 kHz from f_{hf} (bottom panel) that shows a strong overshoot immediately after turn-on.

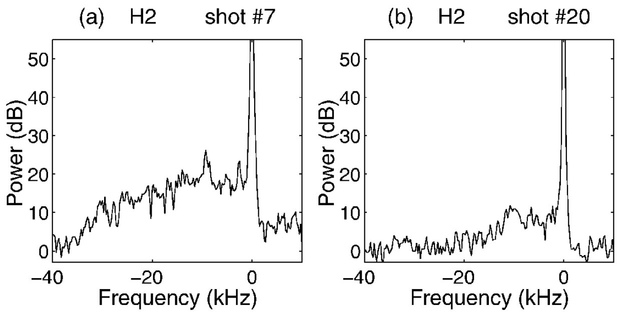

FIG. 6. Frequency spectra of returned hf signal of second pump pulse H_2. Panel (a) shows the spectra during overshoot with strong frequency broadening. Panel (b) shows the spectrum 9 s into heating after broadening has subsided. The frequency scale is offset from f_{hf}.

wave amplitude of $\mathcal{E} \sim 0.025$ gives a striation depth of $\sim 1.5\%$ which is within previous estimates and observations [3,5,19]. For comparison, the scaled main pump wave amplitude is $\mathcal{E} \sim 0.4$. Third, the model predicts the continuum feature requires a higher excitation threshold. This is demonstrated by comparing SEE spectra of H_1 and H_2 with spectra from T_2 (and T_3). In general, superposed spectra with both down-shifted maximum and broad continuum are observed during main heating, while discrete down-shifted maximum with very little broad continuum are observed with the test waves. Fourth, the model predicts that cavitation can occur within striations which leads to a very broad continuum. This appears to be demonstrated from the observation of strong overshoot of the continuum feature with H_2 after preconditioning. The highly nonstationary behavior and the associated wideband spectra agree with general features of cavitation [30]. Further experiments and modeling are needed to confirm this point.

In summary, we have studied the nonlinear physics of SEE and have confirmed the correlation between striations, trapped upper hybrid decay instability, and SEE through our controlled preconditioning experiment. We have demonstrated unambiguously that, in a preconditioned ionosphere with striations, the down-shifted maximum feature can be excited and observed readily with test hf pulses that are 24 dB weaker in power density than the main hf pump wave that preconditions the ionosphere. The results also compare well with predictions from a recent theoretical model of SEE generation via trapped upper hybrid decay instability and cavitation within striations.

This research was supported by ONR Contract No. N00014-96-C-0040, NSF Grant No. PHY-9421693, and partially supported under the auspices of DOE by LLNL Contract No. W-7405-ENG-48. One of the authors (P. Y. C.) acknowledges useful discussions with Dr. Thomas Leyser.

[1] A. Y. Wong, J. Santoru, and G. Sivjee, J. Geophys. Res. **86**, 7718 (1981).
[2] P. A. Fialer, Radio Sci. **9**, 923 (1974).
[3] J. Minkoff, P. Kugelman, and I. Weissman, Radio Sci. **9**, 941 (1974).
[4] S. T. Noble and F. T. Djuth, J. Geophys. Res. **95**, 15 195 (1990).
[5] M. C. Kelley *et al.*, J. Geophys. Res. **100**, 17 367 (1995).
[6] B. Thidè *et al.*, Radio Sci. **18**, 851 (1983).
[7] G. N. Boiko *et al.*, Radiophys. Quantum Electron. **28**, 259 (1985).
[8] B. Thidè *et al.*, J. Geophys. Res. **100A**, 23 887 (1995).
[9] P. Stubbe *et al.*, J. Geophys. Res. **89**, 7523 (1984).
[10] P. Stubbe *et al.*, J. Geophys. Res. **99**, 6233 (1994).
[11] T. B. Leyser *et al.*, J. Geophys. Res. **95**, 17 233 (1990).
[12] T. B. Leyser *et al.*, J. Geophys. Rev. **99**, 19 555 (1994).
[13] H. Derblom *et al.*, J. Geophys. Res. **94**, 10 111 (1989).
[14] W. T. Armstrong *et al.*, Radio Sci. **25**, 1283 (1990).
[15] M. Waldenvik, Ph.D. thesis, Swedish Institute of Space Physics, Uppsala, Sweden, 1994.
[16] P. Bernhardt *et al.*, Phys. Rev. Lett. **72**, 2879 (1994).
[17] T. B. Leyser, Geophys. Res. Lett. **18**, 408 (1991); Phys. Plasmas **1**, 2003 (1994).
[18] E. Mjølhus, J. Atmos. Terr. Phys. **55**, 907 (1993).
[19] A. V. Gurevich, A. V. Lukyanov, and K. P. Zybin, Phys. Lett. **206A**, 247 (1995); V. Gurevich, K. P. Zybin, and A. V. Lukyanov, Phys. Rev. Lett. **75**, 2622 (1995).
[20] Ya. N. Istomin and T. B. Leyser, Phys. Plasmas **4**, 817 (1996).
[21] S. M. Grach *et al.*, Phys. Rev. Lett. **78**, 883 (1997).
[22] E. Mjølhus and E. Helmersen, in *Strong Microwaves in Plasmas*, edited by A. G. Litvak (Institute of Applied Physics, Nizhny Novgorod, 1997), Vol. 2, p. 449.
[23] E. Mjølhus, J. Geophys. Res. (to be published).
[24] A. Y. Wong *et al.*, Phys. Rev. Lett. **63**, 271 (1989).
[25] A. Y. Wong *et al.*, Bull. Am. Phys. Soc. **42**, 1889 (1997).
[26] A. Y. Wong *et al.*, Radio Sci. **25**, 1269 (1990).
[27] K. N. Graham and J. A. Fejer, Radio Sci. **11**, 1057 (1990).
[28] T. B. Jones, T. Robinson, P. Stubbe, and H. Kopka, J. Atmos. Terr. Phys. **46**, 147 (1984).
[29] E. Mjølhus, J. Geophys. Res. **90A**, 4269 (1985).
[30] P. Y. Cheung *et al.*, Phys. Rev. Lett. **79**, 1273 (1997).